Mapping the topological phase diagram of multiband semiconductors with supercurrents (arXiv:1309.2239)

Pablo San-Jose, Elsa Prada, and Ramón Aguado

September 24, 2013

We show that Josephson junctions made of multiband semiconductors with strong spin-orbit coupling carry a critical supercurrent I_c which contains information about the non-trivial topology of the system. In particular, we find that the emergence and annihilation of Majorana bound states in the junction is reflected in strong even-odd effects in I_c under specific conditions. *This effect allows for a direct mapping between the critical supercurrent and the topological phase diagram of the junction, thus providing a dc measurement of the nontrivial topology, despite the absence of a 4π effect in the steady state.*

For realistic junctions (finite size, quasiparticle poisoning) 4π periodicity is always transient and true steady state is always 2π periodic.

- Introduction
  - Topological superconductor
  - Even-odd effect
- Calculations and results
  - Josephson junction with two semi-infinite wires
  - Results
- Implications and Summary

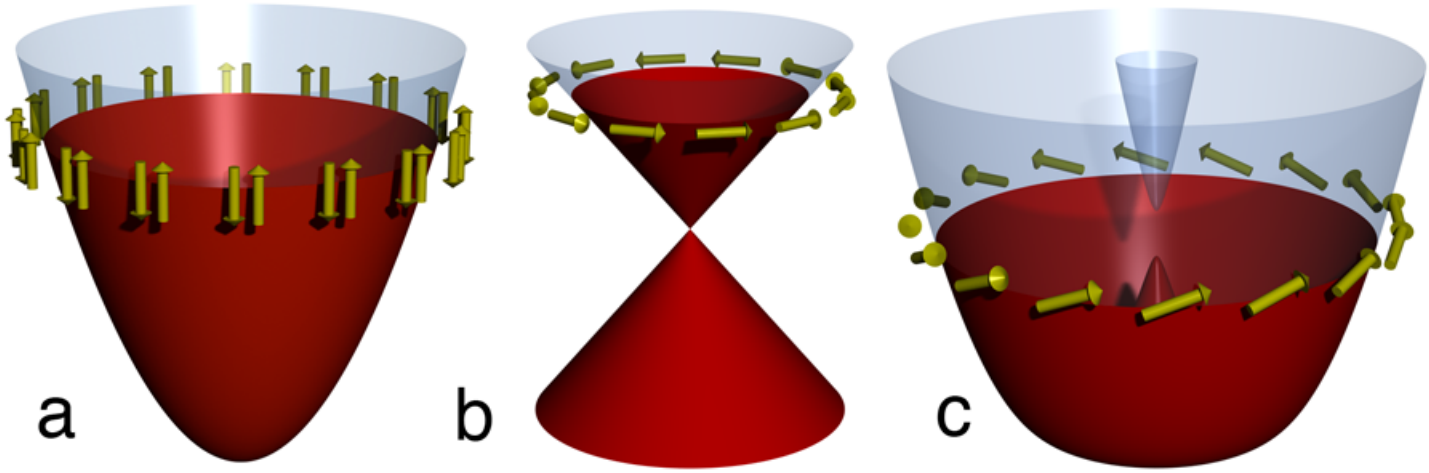

Figure: (a) Parabolic dispersion characteristic of a 2D electron gas with negligible spin-orbit coupling. For each momentum k there are two degenerate spin projections. In this case, electrons must be paired with an unconventional spin-triplet px+ipy order parameter to produce a topological superconductor. (b) Helical liquid on the surface of a topological insulator characterized by Dirac energy dispersion. There is one spin state at each momentum k with orientation perpendicular to k. An ordinary s-wave pairing leads to topological superconductivity. (c) 2D electron gas with strong spin-orbit coupling in the presence of ferromagnetic insulator or in-plane magnetic field. The upward canting of spins signifies broken time-reversal invariance

$H = H_0 + H_Z$

$H_0 = \int d^2\mathbf{r}\psi^\dagger \left[-\frac{\nabla^2}{2m} - \mu - i(\alpha_y\sigma^x\partial_y - \alpha_x\sigma^y\partial_x)\right]\psi$

$H_Z = \int d^2\mathbf{r}\psi^\dagger[V_z\sigma^z]\psi$

Eigenstates are $\psi_\pm$, $\epsilon_\pm(k) = \frac{k^2}{2m} - \mu \pm \sqrt{V_z^2 + \alpha_{SO}^2 k^2}$

$\alpha_x = \alpha_y = \alpha_{SO}$

Topological superconductor

Proximity coupling to *s*-wave superconductor

$$H_{SC} = \int d^2\mathbf{r}[\Delta\psi_\uparrow^\dagger\psi_\downarrow^\dagger + h.c.]. \tag{1}$$

Rewriting H_{SC} in terms of $\psi_\pm$ (eigenstates of H) yields

$$H_{SC} = \int d^2\mathbf{k}\Big[\Delta_{+-}(k)\psi_+^\dagger(\mathbf{k})\psi_-^\dagger(-\mathbf{k}) + \Delta_{--}(\mathbf{k})\psi_-^\dagger(\mathbf{k})\psi_-^\dagger(-\mathbf{k}) + \Delta_{++}(\mathbf{k})\psi_+^\dagger(\mathbf{k})\psi_+^\dagger(-\mathbf{k}) + h.c.\Big], \tag{2}$$

with

$$\Delta_{+-}(k) = \frac{V_z}{\sqrt{V_z^2 + \alpha_{SO}^2 k^2}}\Delta \tag{3}$$

$$\Delta_{++}(\mathbf{k}) = \frac{-\alpha}{2\sqrt{V_z^2 + \alpha_{SO}^2 k^2}}\left(k_y + ik_x\right)\Delta \tag{4}$$

$$\Delta_{--}(\mathbf{k}) = \frac{-\alpha}{2\sqrt{V_z^2 + \alpha_{SO}^2 k^2}}\left(k_y - ik_x\right)\Delta. \tag{5}$$

The proximity effect thus generates not only interband s-wave pairing encoded in the first term, but also *intra*band $p_x \pm ip_y$ pairing with opposite chirality for the upper/lower bands. $V_Z \gg \sqrt{\Delta^2 + \mu^2}$

- System becomes topologically nontrivial if $V_Z \gg \sqrt{\Delta^2 + \mu^2}$ and develops chiral channels along its boundaries.
- In a quasi-1D geometry (with multiple discrete confinement subbands), this picture is replicated for each subband independently (each band has its own critical $V_Z^{(n)} = \sqrt{\Delta^2 + \mu_n^2}$, with μ_n being the Fermi energy measured from the bottom of each subband).

- Coupled bands lead to hybridization of Majorana modes into full fermions at non zero energy resulting in *even-odd* effect.
- Transverse spin-orbit coupling α_y is an intrinsic source of subband mixing (subband spacing E_{sb} depends upon W).
- $\frac{E_{SO}}{E_{sb}} = (4/3\pi)^2 \frac{W}{l_{SO}}$, $l_{SO} \equiv \hbar^2/m\alpha_y$

Multiple Bands-even odd effect

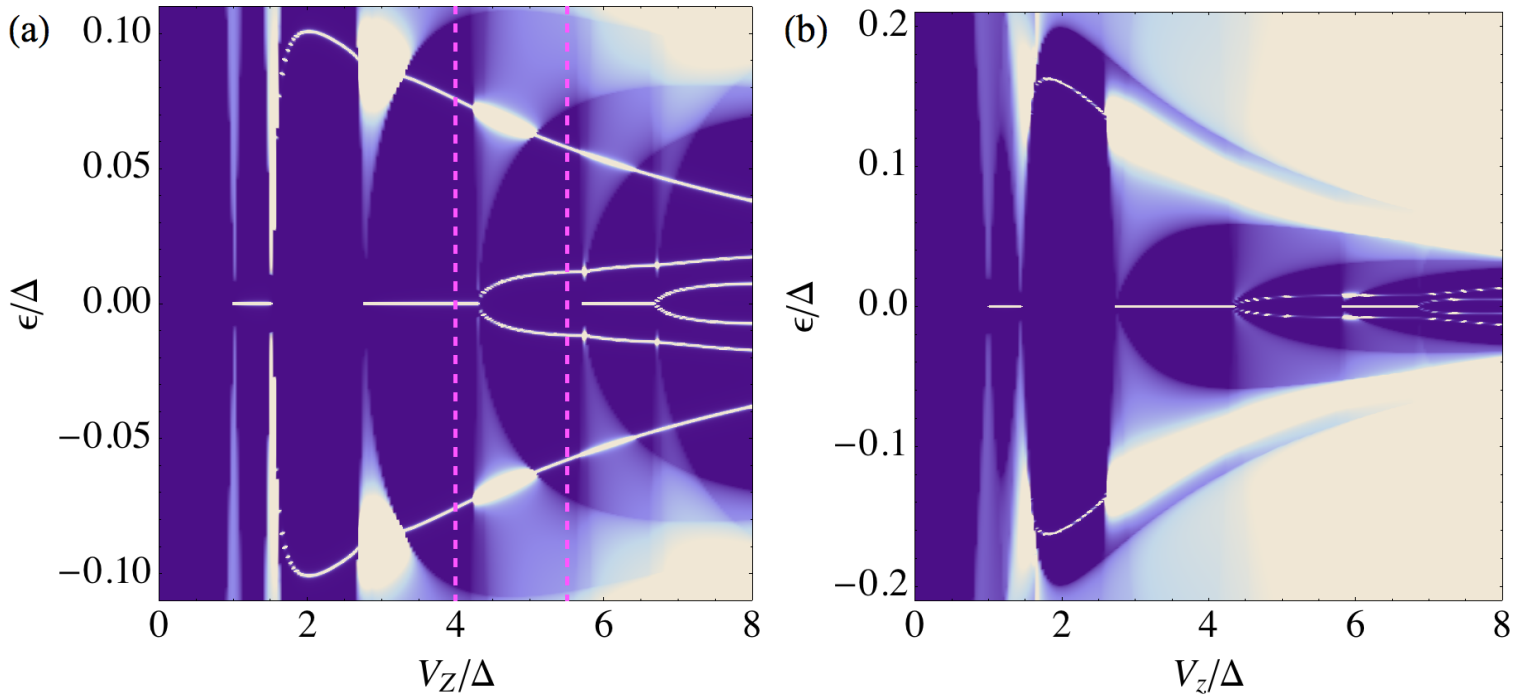

Figure: Local density of states at the end of a semi-infinite multimode wire at the point of depletion $\mu = 0$, as a function of Zeeman splitting V_Z . Blue is zero, and white is maximum. The zero energy states follow an even-odd pattern. Panel (a) corresponds to $W/l_{SO} = 1.9$, and (b) $W/l_{SO} = 3.1$. The latter shows a merging of the hybridized highest Majorana states and the continuum.

- Josephson junction of two semi-infinite multimode wires with superconducting phase difference ϕ, junction length$\to 0$
- Subgap levels $\epsilon_0^{(n)}$ at the ends of the wires hybridize into ABSs across the junction $\epsilon_\pm^{(n)}(\phi) \approx \epsilon_0^{(n)} \pm E_T^{(n)} \cos(\phi/2)$

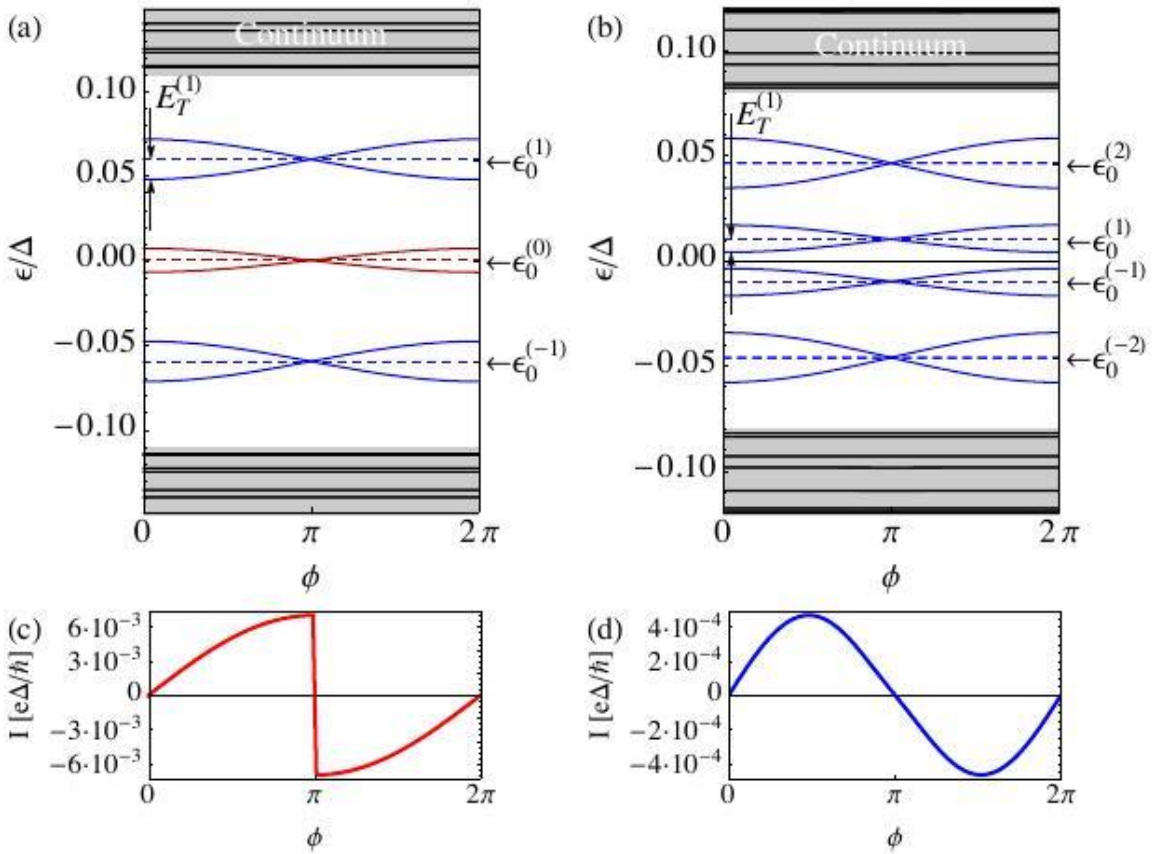

Figure: Subgap energy levels of a multimode Josephson junction as a function of phase difference ϕ. Zeeman field is $V_Z = 4\Delta$ (a) and $V_Z = 5.5\Delta$ (b), corresponding to dashed lines in Fig. 1(a). The sub-gap levels $\epsilon_0^{(n)}$ at the ends of the decoupled wires (dashed) hybridize across the junction into ϕ-dependent ABSs (solid) of amplitude $E_T^{(n)}$. Josephson currents associated to (a) and (b) are shown in (c) and (d) respectively, including 200 levels in the quasicontinuum [black lines in (a,b)].

- $I(\phi) = I_{qp} - \frac{1}{2}\frac{e^2}{\hbar}\sum_{n,s=\pm}\tanh\left[\frac{\epsilon_s^{(n)}(\phi)}{2k_BT}\right]\partial_\phi\epsilon_s^{(n)}(\phi)$
- If $E_T^{(n)} < \epsilon_0^{(n)}$, zero temperature contribution to $I(\phi)$ (and I_c), of $\epsilon_+^{(n)}$ and $\epsilon_-^{(n)}$ approximately cancels for any $n > 0$
- Ignoring I_{qp} background

$$I_c \approx \begin{cases} 0 & \text{if } N\text{mod}2 = 0 \\ \frac{1}{2}E_T^{(0)} & \text{if } N\text{mod}2 = 1 \end{cases} \tag{6}$$

- Corrections to even odd effect large $E_T^{(n)}$, disorder, finite length of semiconductors or the junction

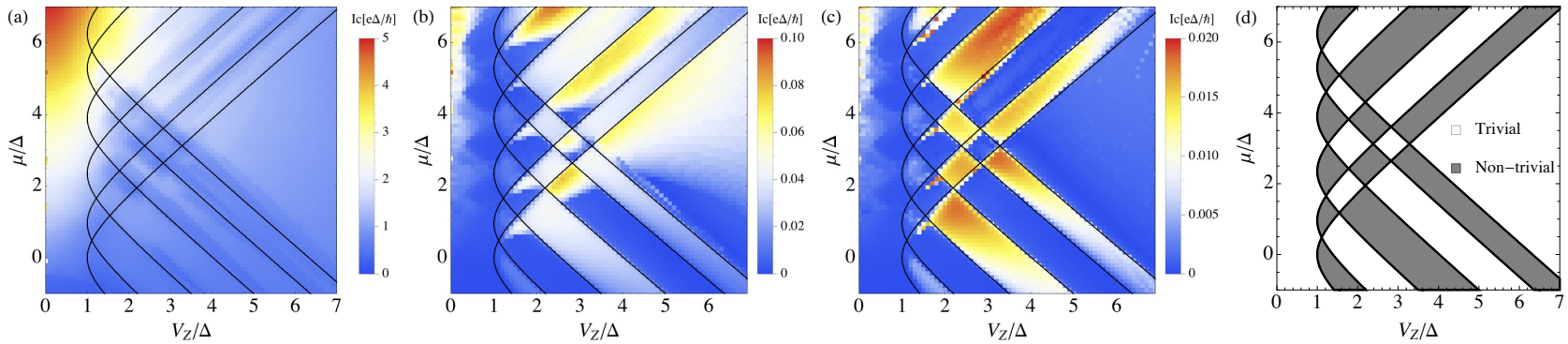

Figure: (a-c) Critical supercurrent versus Fermi energy μ and Zeeman field V_Z for a multimode Josephson junction at three different transparencies, corresponding to $E_T^{(1)} > \epsilon_0^{(1)}$ [panel (a)], $E_T^{(1)} \sim \epsilon_0^{(1)}$ [panel (b)] and $E_T^{(1)} < \epsilon_0^{(1)}$ [panel (c)]. Black lines correspond to critical fields $V_Z^{(n)}$. Note the marked even-odd effect in (c). (d) shows the corresponding topological phase diagram (white is even, gray is odd).

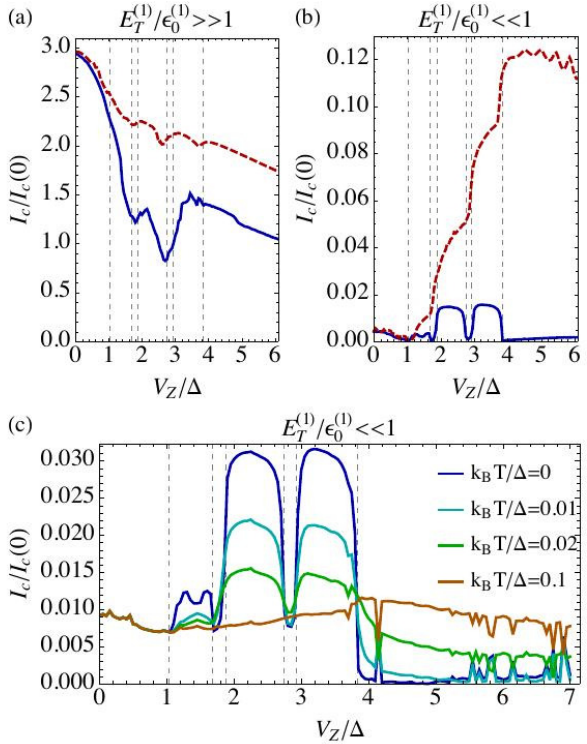

Figure: Zero temperature critical supercurrent versus Zeeman field V_Z for a multimode Josephson junction for $E_T^{(1)} > \epsilon_0^{(1)}$ [panel (a)] and $E_T^{(1)} < \epsilon_0^{(1)}$ [panel (c)]. In both cases, the Fermi energy $\mu = 3.7\Delta$. Solid (blue) curves correspond to $W/l_{SO} = 1.9$ and dashed (red) ones to $W/l_{SO} \to 0$. Vertical dashed lines mark the positions of the critical fields V_Z^n . The temperature dependence of the solid blue curve in (b) is shown in (c), including a portion of the continuum contribution I_{qp} (note the current background respect panel (b), where I_{qp} was ignored).

- In conclusion, we have shown that the topological order in Rashba semiconductors with induced superconductivity, that is known to manifest in a spectral even-odd effect for the number of protected Majorana zero modes at the end of quasi-1D geometries, also produces a strong signature in the critical supercurrent of multimode Josephson junctions.
- Even in the presence of real-world imperfections and finite temperature, the difference in critical current between a non-trivial odd phase (a single Majorana pair in the junction), and a trivial even phase, is expected to be rather large in a small transparency regime.